

X17952

UNCLASSIFIED

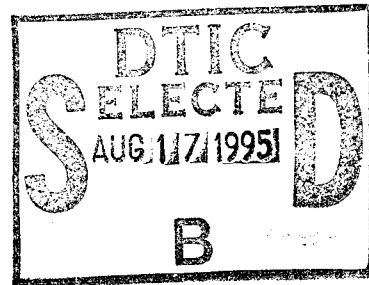
UCRL-2297

Subject Category: PHYSICS

UNITED STATES ATOMIC ENERGY COMMISSION

SPIRAL BEAM ACCELERATOR MODEL  
RESULTS

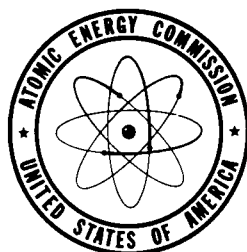
By  
Stirling A. Colgate  
A. J. Schwemin



July 1953

Radiation Laboratory  
University of California  
Berkeley, California

Technical Information Extension, Oak Ridge, Tennessee



UNCLASSIFIED

DTIC QUALITY INSPECTED 5

19950815 050

Date Declassified: March 2, 1956.

**LEGAL NOTICE**

This report was prepared as an account of Government sponsored work. Neither the United States, nor the Commission, nor any person acting on behalf of the Commission:

A. Makes any warranty or representation, express or implied, with respect to the accuracy, completeness, or usefulness of the information contained in this report, or that the use of any information, apparatus, method, or process disclosed in this report may not infringe privately owned rights; or

B. Assumes any liabilities with respect to the use of, or for damages resulting from the use of any information, apparatus, method, or process disclosed in this report.

As used in the above, "person acting on behalf of the Commission" includes any employee or contractor of the Commission to the extent that such employee or contractor prepares, handles or distributes, or provides access to, any information pursuant to his employment or contract with the Commission.

This report has been reproduced directly from the best available copy.

Issuance of this document does not constitute authority for declassification of classified material of the same or similar content and title by the same authors.

Printed in USA, Price 25 cents. Available from the Office of Technical Services, Department of Commerce, Washington 25, D. C.

AEC, Oak Ridge, Tenn.

UCRL-2297

UNIVERSITY OF CALIFORNIA  
Radiation Laboratory  
Contract No. W-7405-eng-48

SPIRAL BEAM ACCELERATOR MODEL RESULTS

Stirling A. Colgate and A. J. Schwemin

July, 1953

Berkeley, California

Accordance For	
TYPE	DATA
DATA	DATA
UNCLASSIFIED	DATA
Classification	DATA
DATA	
Distribution/Conf.	
Availability Codes	
DATA	DATA and/or
DATA	DATA
A-1	

SPIRAL BEAM ACCELERATOR MODEL RESULTS

Stirling A. Colgate and A. J. Schwemin

Radiation Laboratory, Department of Physics  
University of California, Berkeley, California

July, 1953

ABSTRACT

A model of the spiral beam accelerator or beam buncher has been made -- full scale in dimensions but reduced in current and voltages. The basic result of the model was an accelerator with  $60 \pm 5$  percent phase acceptance under conditions of central rod potential, angular momentum, and transit time factor considerably more modest than originally conceived. The bunching and beam stability were similarly favorable.

SPIRAL BEAM ACCELERATOR MODEL RESULTS

Stirling A. Colgate and A. J. Schwemin

Radiation Laboratory, Department of Physics  
University of California, Berkeley, California

July, 1953

INTRODUCTION

The spiral beam accelerator originated from the need for a phase stable linear accelerator to be used in the low voltage region up to 1 Mev capable of handling large currents - up to 10 amps, having a large phase acceptance - up to 100 percent, and giving a beam well bunched in velocity and space for injection into another accelerator. The proposed method of doing this was to introduce charge in the form of a central rod (50 to 100 kilovolts negative) in the center of the beam, the rod being coaxial with the drift tubes of an ordinary Sloan-Lawrence type linear accelerator. By giving the accelerated particles angular momentum around the central rod (in addition to their axial motion) a stable "Kepler orbit" is established that prevents the particles from striking the inner central rod or outer coaxial drift tubes. The particles execute helical orbits around the central rod and are well confined between a minimum and a maximum radius by the d. c. potentials involved. The details of the orbit - stability, shape, current density, and susceptibility to perturbations are discussed in detail in report UCRL-1820. This report describes an experimental model test of the theory.

The basic result of the model was an accelerator with  $60 \pm 5$  percent phase acceptance under conditions of central rod potential, angular momentum, and transit time factor considerably more modest than originally conceived. The bunching and beam stability were similarly favorable.

The model was designed to be full scale in dimensions and frequency for a buncher for Mark I, but with low current and the voltages scaled by one-half. This gave the following conditions:

1. Bore diameter: 6 in.
2. Central rod diameter: 3/4 in.
3. Frequency: 12.6 megacycles
4. Ratio of gap to cell length: 0.2
5. Constant voltage gain per gap: 10 kv
6. Central rod voltage: 50 kv
7. Injection voltage: 25 kv
8. Twelve drift tubes giving a final energy of 120 kv.

Limitations in the original design of the model caused a modification in items 6 and 7. The peak central rod voltage attainable was 40 kv, and the injection energy was 10 to 15 kv depending upon angular momentum. These two limitations were a product of the space requirements and practical control range of a beam mass spectrometer at the injection point and had no bearing on inherent limitations of the spiral accelerator.

#### GENERAL MECHANICAL AND ELECTRICAL DESCRIPTION OF BUNCHER

The twelve drift tubes of the accelerator had an outside diameter of 6 in. with 1/8 in. walls, (Figs. 1 and 2) supported by copper tabs alternately attached to either of two horizontal supporting rods 2 in. in diameter. These horizontal support rods formed the drift tube rf feed lines, and were connected to two vertical stems of the same diameter that went through the vacuum tank wall through two large ceramic insulators. These stems in turn were shorted and grounded at an appropriate point (about 4 feet above the tank) such as to make the two stems (with supporting rods and drift tubes) resonate against one another at 12.6 megacycles. This rf design by the first author was not satisfactory but fortunately the requirements of the system were sufficiently modest. (The whole resonant loop should have been inside the vacuum in order to minimize

losses.) The vertical stems were fed cw from a 10 kw oscillator at the proper impedance points, giving 27 kv peak voltage between drift tubes.

Sections of 6 in. diameter industrial glass tubes are mounted in line with the drift tubes on both ends of the machine. The ion source injector with variable controls was mounted in a "T" section while a straight section of glass was used to house the measuring equipment at the exit of the buncher. See Figs. 3 and 4.

A hard drawn copper rod of 3/4 in. outside diameter was placed coaxially down the center of the drift tubes and extended from the injector to the exit of the buncher. This rod was supported by a high voltage insulator on the injector end, and a formed piece of 3/16 in. glass rod in a "V" configuration at the exit end of the buncher. The rod itself had a slight pre-set bend to compensate for sag between the two end supports. The central rod was terminated in a round polished brass plug at the exit end and a ceramic insulator on the injector end. An rf choke was mounted inside the central rod at the injector end to keep the rf appearing on the rod from getting into the high voltage power supply.

The injector consisted of an rf ion source, mass spectrometer, focussing electrodes and angular momentum paddle (Fig. 5). Since the injector is operated at 10 kv above ground, the palladium leak heater, focussing electrode, focussing magnet, and extraction high voltage supply had to be isolated from ground. The angular momentum paddle, beam collection cup, and beam selecting paddles were made adjustable through Wilson seals at the bottom of the "T" section of pipe.

#### GENERAL BEAM CHARACTERISTICS

The beam was a magnetically analyzed proton beam of 10 to 50 microamps about 2 millimeters in diameter at injection. The proton source was 10 kilovolts positive with respect to ground; the beam was magnetically analyzed and separated at ground potential, and then accelerated to the negative central rod potential through the electrode B. (See Fig. 1.) The

beam was deflected azimuthally with respect to the central rod by the field between the adjustable angular momentum paddle (A) at ground potential and the extension of electrode (B) at negative central rod potential. By adjusting the radial distance of the angular momentum paddle from the central rod, the radial velocity at injection could be made zero. This is the condition for a beam orbit of minimum outside radius. The inside radius (as discussed in UCRL-1820) is determined by the angular momentum, and this in turn was varied by adjusting the azimuthal distance between paddle A and electrode B. Since the voltage between them was constant (central rod voltage) this changed the field strength and hence the degree of deflection of the beam in the azimuthal direction. The inside minimum beam radius could be varied from 3/8 in. (i.e., grazing the central rod, minimum angular momentum) to 2 in. (a circular orbit at injection radius) which is just dynamically unstable, and is the maximum angular momentum. The injection energy into the rf system is determined by the axial velocity of the beam after it has traveled down the bore a distance equal to approximately the diameter of the bore away from the perturbation of the electrodes (A and B). With no rf, this axial velocity is maintained for the length of the machine until the beam comes within a bore diameter of the exit end. This concept of constant axial velocity (for no rf) throughout the major length of the machine is different from the analysis in report UCRL-1820. There it was erroneously stated that the d. c. beam would lose energy uniformly throughout the length of the machine from an energy of the central rod injection electrode - down to ground of the exit beam cup. It was shown experimentally that the axial velocity was constant (with no rf) by observing visually that the "pitch" of the beam orbit was uniform throughout the length of the machine. For normal conditions of injection, the "pitch" was about one-eighth the total length, or, about 8 inches. When this error was recognized, it caused a change in the injection energy, and so instead of re-instrumenting the proton source, additional drift tubes at the low energy end were added to accept a lower injection energy. This resulted in the final injection energy of 10 to 15 kv for the model.

At an early stage in the model development, no magnetic analysis of the injected beam was used. As a result, the beam was composed principally of heavy ions -  $H_2^+$  and  $C^+$  and  $O_2^+$ , etc. These ions follow the same d. c. trajectories as the  $H^+$  ion, and are much more visible due to their greater ionization. The spiral beam could be observed through the entire length of the machine, and it was at this stage that it was determined that there was no beam loss between injection and the exit end with no rf. The "pitch" of the helical orbit agreed with theory.

#### ACCELERATOR DRIFT TUBE DESIGN

On the basis of electrolytic tank measurements, (described in UCRL-1820) it was determined that a transit time factor of 50 percent was a reasonable estimate for all gaps of the accelerator. For simplicity of the rf circuit, a constant energy gain of 10 kv per gap was chosen and a drift tube table was made accordingly. However, it was not recognized until after the completion of measurements that another assumption had been made, namely that the rf phase at a given instant of time was constant for the entire length of the accelerator. That the latter was not so can be seen from the fact that the drift tube support rods, with drift tubes, act like a loaded line so that the phase at either end of the line is retarded with respect to the center. It is estimated that the phase at the ends of the machine was retarded something like 5 percent with respect to the center. This means that a particle entering the accelerator sees a region of increasing phase so that it must gain more energy than for constant phase, and in the second half, decreasing phase and so less energy gain per gap to stay in step.

This modifies the beginning part of the accelerator so that the protons must gain 11 kv per gap and in the second half only 9 kv. This effect is in the direction to lower the phase acceptance of the accelerator, because the injection end is just where one wants small accelerating voltages and a large synchronous phase angle. In another model, these conditions could readily be obtained.

### PHASE ACCEPTANCE MEASUREMENTS

Phase acceptance is defined as the ratio of accelerated beam current to injected beam current. Because the acceleration was rather modest in the model (110 kv), it was difficult to determine uniquely the difference between accelerated and unaccelerated or injected beam. Magnetic fields were not practical because of the large diameter and divergence (without central rod) of the exit beam. In order to detect the accelerated beam with certainty from particles of lower energy, a beam cup was made with an entrance foil of aluminum 170 micrograms/cm<sup>2</sup> thick. (Fig. 6.) This definitely excluded all particles of less than 65 kv energy, and had a transmission as a function of proton energy as given in Fig. 7. This fractional transmission is due to charge exchange. The first transmission curve was derived from actual measurements on the bevatron Cockcroft-Walton injector, and the second from calculations from charge exchange figures by James A. Philips of Los Alamos and ionization loss figures by Wilcox (Phys. Rev. 74, 1743 (1948)). In the phase acceptance measurements, an accelerated beam energy of 110 kv was assumed. This was based on a later measurement of the beam energy, and gives a correction to the transmitted current of 30 percent.

The injected beam and the exit beam with no rf showed the same current, which implies no beam loss through the length of the accelerator under d.c. conditions. This was checked by using a small Faraday cup to intercept the beam at the injector end and a large cup at the exit end.

With a positive bias of 45 volts or greater on the small injector cup the ratio between injected current and current at the end of the machine were the same. The ratio was constant for the conditions (1) when the small cup was biased, (2) for the full range of angular momentum for stable orbits and (3) for central rod voltage greater than 10 kv. It was not necessary to bias the large cup at the exit end of the buncher because of the high negative central rod voltage which kept the secondary electron emission from the cup from returning to the accelerator or to ground.

Phase acceptance measurements were then made as a function of the rf peak voltage by taking the ratio of the accelerated beam through the foil with rf to the d.c. beam into foil with no rf. Both foil and cup were separately metered at all times.

The phase acceptance as a function of rf voltage with the 30 percent correction for foil transmission for three different central rod voltages is given in Fig. 8. In addition, the phase acceptance was found to be quite independent of angular momentum in the region where the d.c. beam was stable. Changing the angular momentum from maximum to minimum changes the injection energy from 10 to 15 kilovolts.

The fact that some beam was accelerated at an rf voltage of 15 kilovolts, shows that the transit time factor was considerably better than 50 percent, i.e., 75 percent at 15 kilovolts. This could be taken advantage of in another model by decreasing the synchronous phase angle at the higher energy end of the accelerator where the beam is bunched. However, the peak phase acceptance occurred at 20 kilovolts, which agrees with an estimated 50 percent transit time factor near the injector end.

#### ENERGY SPECTRUM OF THE ACCELERATED BEAM

Since the accelerated beam diverges quite rapidly after leaving the field of the central rod and is spread into a large donut shaped beam, magnetic analysis of the energy is very difficult. To overcome this diverging effect, it was decided to analyze small sections of the beam at a time. To do this, a phosphor plate was made so that it was adjustable and sections of the accelerated beam were tracked for several inches and recorded. From this information, a small torroidal deflection magnet was made to fit inside the exit glass section with the pole tips following the plotted path of the beam. (Figure 9.) A grounded metal plate with a phosphor covering the front side was secured to the bending magnet. Another similar phosphorized plate with accurate vertical and horizontal calibrations was placed to the rear of the magnet, and 1/8 in. aperture was drilled in the masking plate so that a small section of the beam would enter between the deflection magnet pole pieces. With this apparatus, different sections of the beam were analyzed to determine the energy and the energy spread of the beam. The magnet was calibrated by the magnet group before tests were run.

The energy spectrum of the accelerated beam was monoenergetic to  $\pm 5$  percent which agrees with the estimate made of the bunching in velocity that should take place for 12 drift tubes. The absolute energy of the beam was not determined as accurately, but lay between 90 to 110 kilovolts. There was a component of the beam small in magnitude that had an energy of 65 kilovolts, but this was not included in the phase acceptance measurements because of the small foil transmission at this energy.

#### BUNCHING MEASUREMENTS

To obtain information on bunching, several different methods were used and results compared. The first method tried made use of a Faraday cup, which fed a 955 cathode follower amplifier. This then ran into a 300 ohm coax line to a 517 Tektronix Scope. Because of the small beam current, enough signal could not be secured to give adequate results. Amplification of the signal was limited by the large amount of pickup in the equipment and lines from rf from the drift tube oscillator and rf on the ion source chamber.

A second method employed the generation of X-rays proportional to the beam current which were detected with a scintillation detector. The X-ray generator was a lattice build up of brass strips, with a retarding grid in the front and an accelerating grid in the rear. (See Fig. 10.) The beam striking the lattice produced secondary electrons which were then focussed and accelerated through a 50 kv d. c. field onto a 0.001 in. molybdenum foil. Some of the X-rays thus produced struck a stilbene crystal at the end of a light pipe leading to a 5819 photomultiplier. The signal was fed from the multiplier to a 517 Tektronix scope. This method worked well, but was hard to photograph because of the sweep jitter in the scope over the many sweeps required to get a clear photograph. (See Figs. 11 and 12.)

A different method of sweeping the scope was used to resolve information from the counter. An rf pickup loop was coupled from the drift tube oscillator and directly to the scope deflection plates presenting a circular sweep, (Fig. 13). The peak on the left corresponds to the bunch.

A visual analysis of single scope traces gave the result that the beam was bunched in a current versus time picture of  $40^{\circ}$  full width at half maximum out of  $360^{\circ}$ , or approximately a 10 percent bunch. This was measured at a distance of two cell lengths from the last gap, so that this observed bunching indicated a velocity spread of less than 5 percent, or an energy full width of less than 10 percent. This is in agreement with the previous measurement of energy spread.

#### EFFECT OF RADIAL SUPPORTS OF THE CENTRAL ROD

If a central rod accelerator is to be used for considerable lengths, it is evident that some type of support for the central rod must be provided. With this in mind, radial perturbations were introduced at the injector end and at the exit end of the accelerator.

At the injector end, the perturbation is most serious. Here, it was determined experimentally that a radial rod from the central rod, removes approximately 15 percent of an azimuthally symmetric beam. At the high voltage end the amount removed was about 5 percent. These results agree with the concept that the perturbation is effective in loosing beam if the perturbing field extends axially over a region where the beam changes radius by a large fraction. The perturbation of a radial support extends over an axial region equal to approximately the diameter of the bore. At the low voltage end of the accelerator, the "pitch" of the helical orbit is equal to 2.5 diameters; at the high energy end the pitch is equal to 7.5 diameters. If the energy of the beam were increased to the point where central rod supports were needed, the field perturbation would become negligible and the beam loss would be the geometrical area of the support.

#### CONCLUSION AND SCALING LAWS

The principle advantages of the spiral beam accelerator are:

1. For no rf, the radial stability is independent of axial velocity, so that the stability at the injection end can be made correspondingly large by keeping the rf fields small.

2. The presence of the negative central rod neutralizes to first order the effects of space charge defocussing by introducing charge into the center of the beam.

3. The physical bulk of the stabilizing system (central rod) is small and scales as the axial velocity. This means that the interelectrode capacity is kept small at the low voltage end of the accelerator, and thus the power requirements are reduced.

4. Since the power requirements of the stabilizing system are negligible, drift spaces of any convenient length can be used between various sections of an accelerator, provided debunching is not a problem.

5. The exit beam is donut shaped in cross section. This can be either an advantage or disadvantage, depending upon application.

6. The stability conditions are non-critical to either electrical or mechanical changes.

To take advantage of these characteristics, the following approximate design criteria can serve as a guide.

1. The energy gain per gap for large phase acceptance should be approximately one-third of the central rod voltage at the injection end. After four or five drift tubes the energy gain per gap can be considerably increased provided the synchronous phase angle is correspondingly decreased. This corresponds to the beam being bunched and then crossing the gap at a time of small net radial forces.

2. A larger product of frequency times bore diameter times the square root of the central rod voltage should give better phase acceptance, because it makes the percentage change in beam radius per cell length smaller, and consequently, the change in radial energy smaller. For example, an accelerator with a 2 in. bore diameter, 48 megacycle and 50 kv on the central rod would give 2 Mev in about 20 ft. feet length.

3. The maximum practical energy for such an accelerator is determined by the criterion that the maximum drift tube length should be less than two or three bore diameters. This implies that the capacity to the central rod of each drift tube be less than the capacity to the adjoining drift tubes, i. e., the circulating current losses due to the central rod are small.

By increasing the frequency up to 48 megacycles, changing frequency for higher energy end of the machine, and using as many as six phases instead of two, the energy could be taken up to 100 Mev. This would still imply four or five drift tubes per stem so that power losses would be correspondingly low. There is apparently no need for phasing of rf at points of frequency change along the length of such an accelerator because the phase match can be made by a region of low rf field gradient (four or five drift tubes) at the new frequency, adiabatically shifting and chopping the beam bunch into a new phase.

This ability of changing frequency at will at any point with no beam loss and no phase matching would be useful for injecting into a very high frequency accelerator. The usual alternative for high frequency injection are:

1. Very short drift tubes with large field interpenetration and corresponding poor efficiency or -
2. An increased cell lenght of  $\beta\lambda = 3/2$  or greater, implying more rf power for a given final energy.

The spiral accelerator on the other hand, could be used to accelerate at a lower frequency and then shift to a higher frequency after an energy of 1 to 10 Mev had been attained. The high frequency beam would be partially modulated with the injection frequency.

#### ACKNOWLEDGMENT

The spiral beam accelerator, or beam buncher, was conceived of while the first author was working under the direction of Sumner Kitchen in the spring of 1952. It was largely Dr. Kitchen's personal encouragement that forced the theoretical work to completion. The need for a practical model was recognized by Dr. L. W. Alvarez, and by his authorization, work was begun in the summer of 1952. Late in the summer of 1952 the second author took over the construction and operation of the model. Mr. Douglas Parmentier aided him throughout the study.

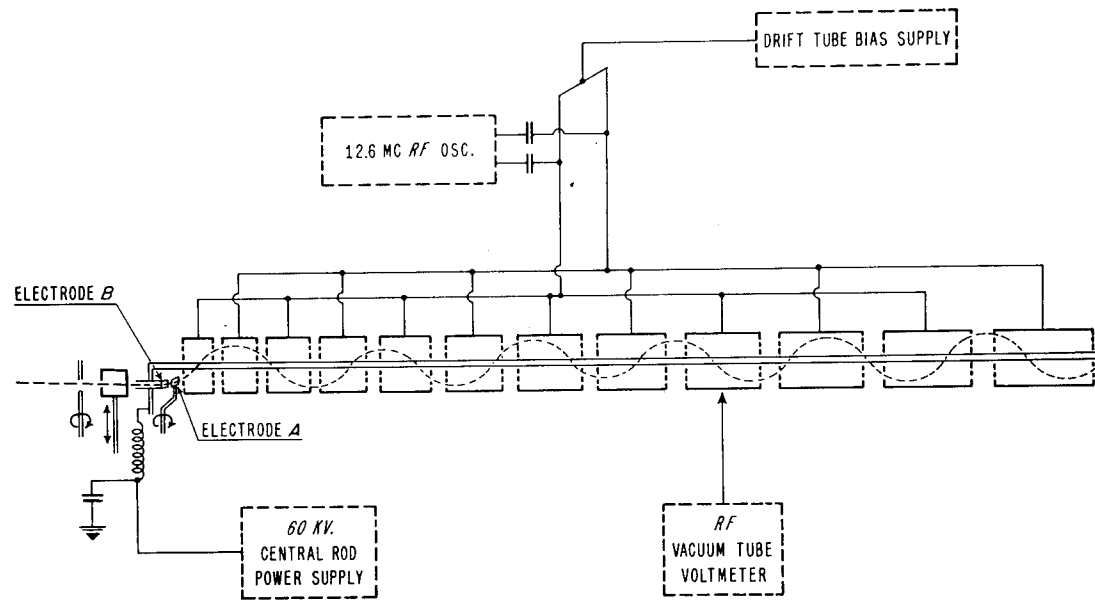
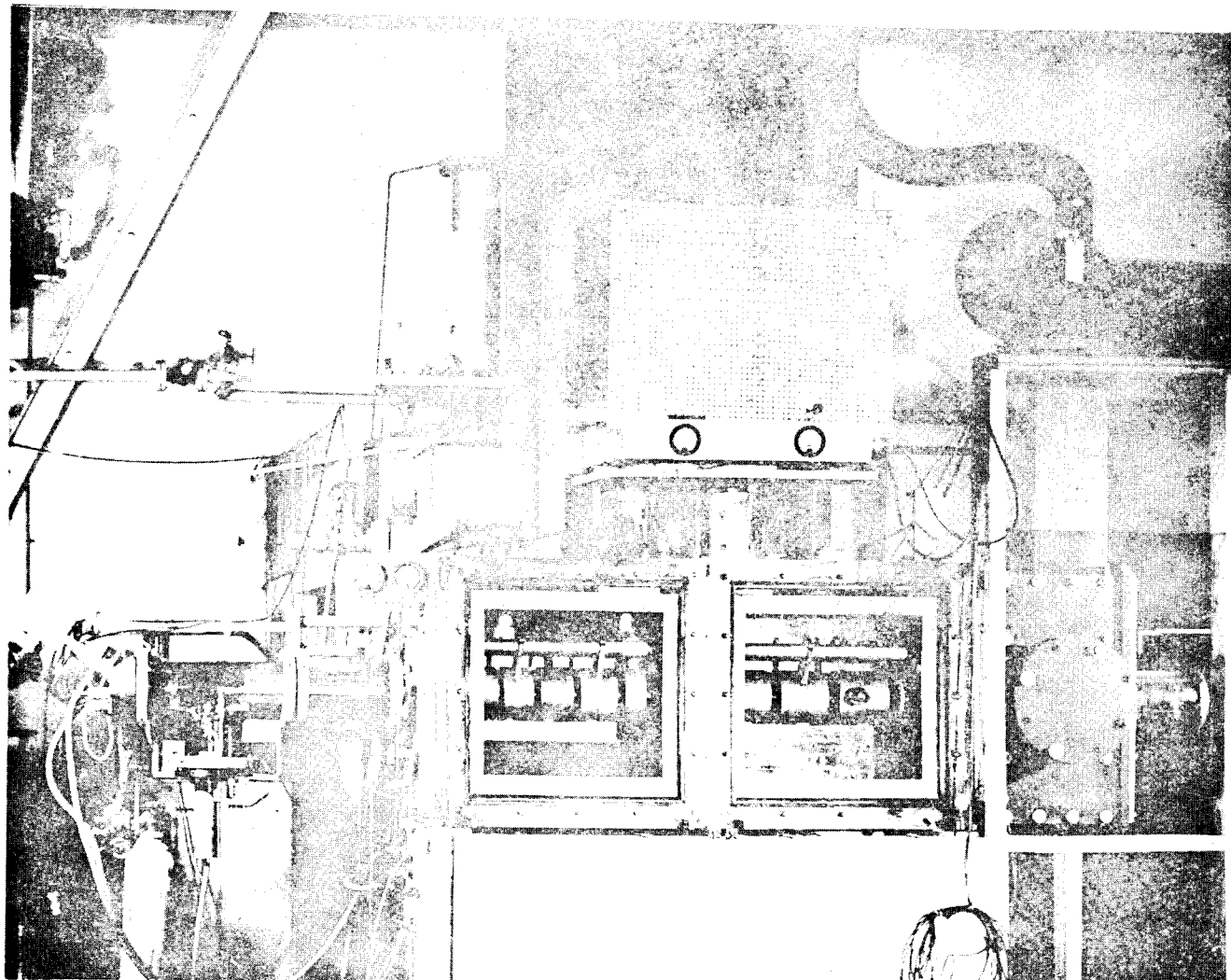


Fig. 1



ZN-693

Fig. 2. The beam buncher.

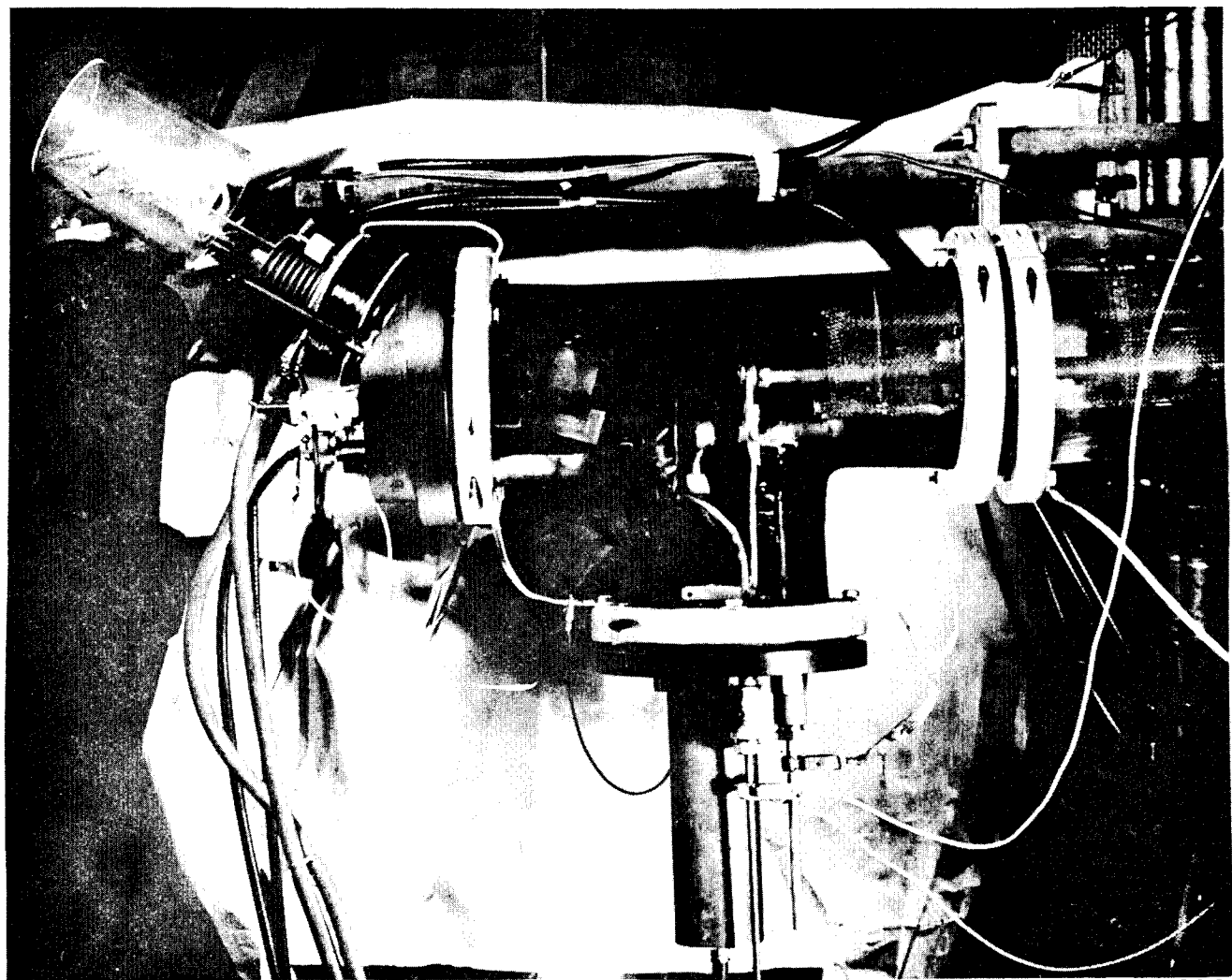


Fig. 3. The ion source end.

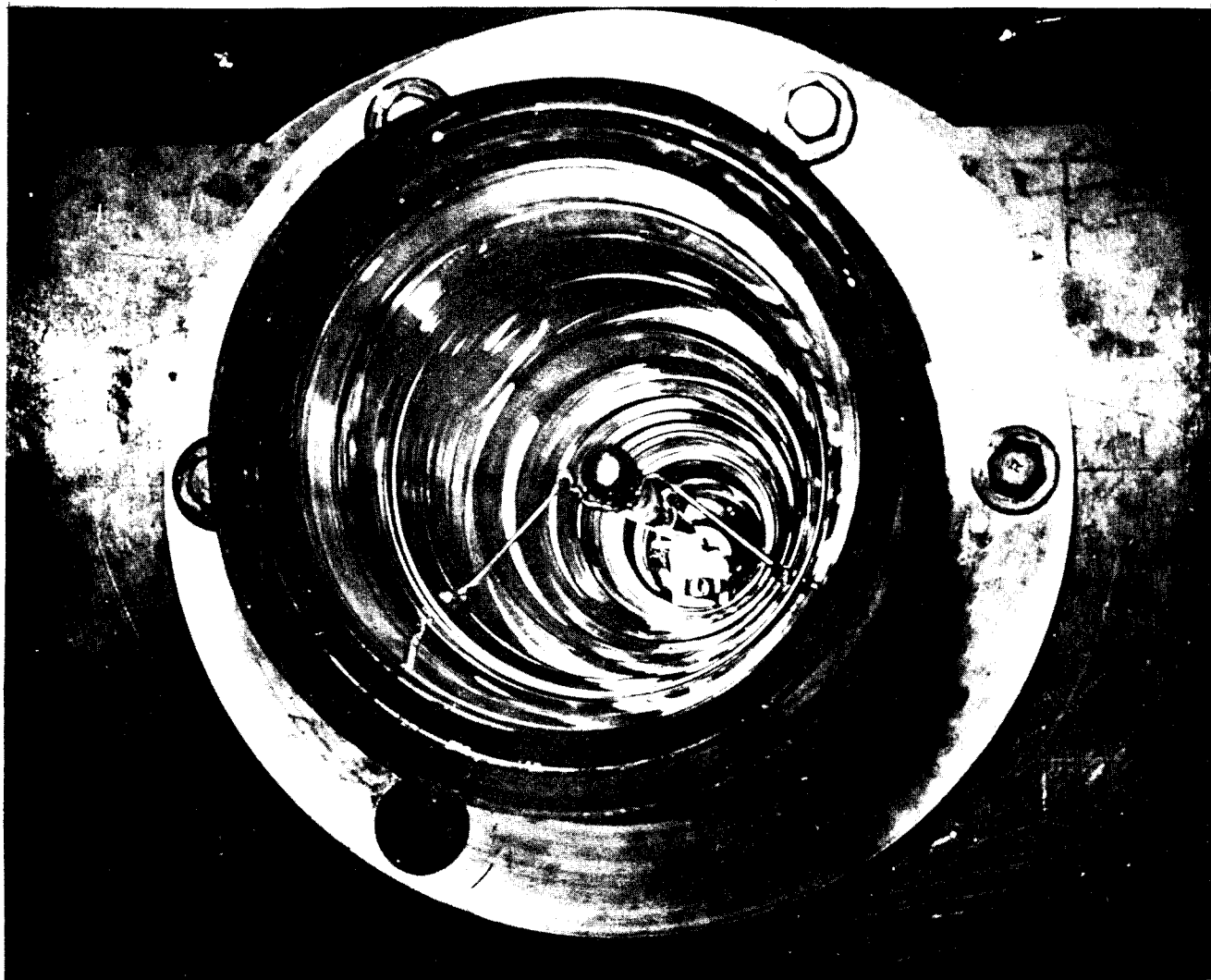
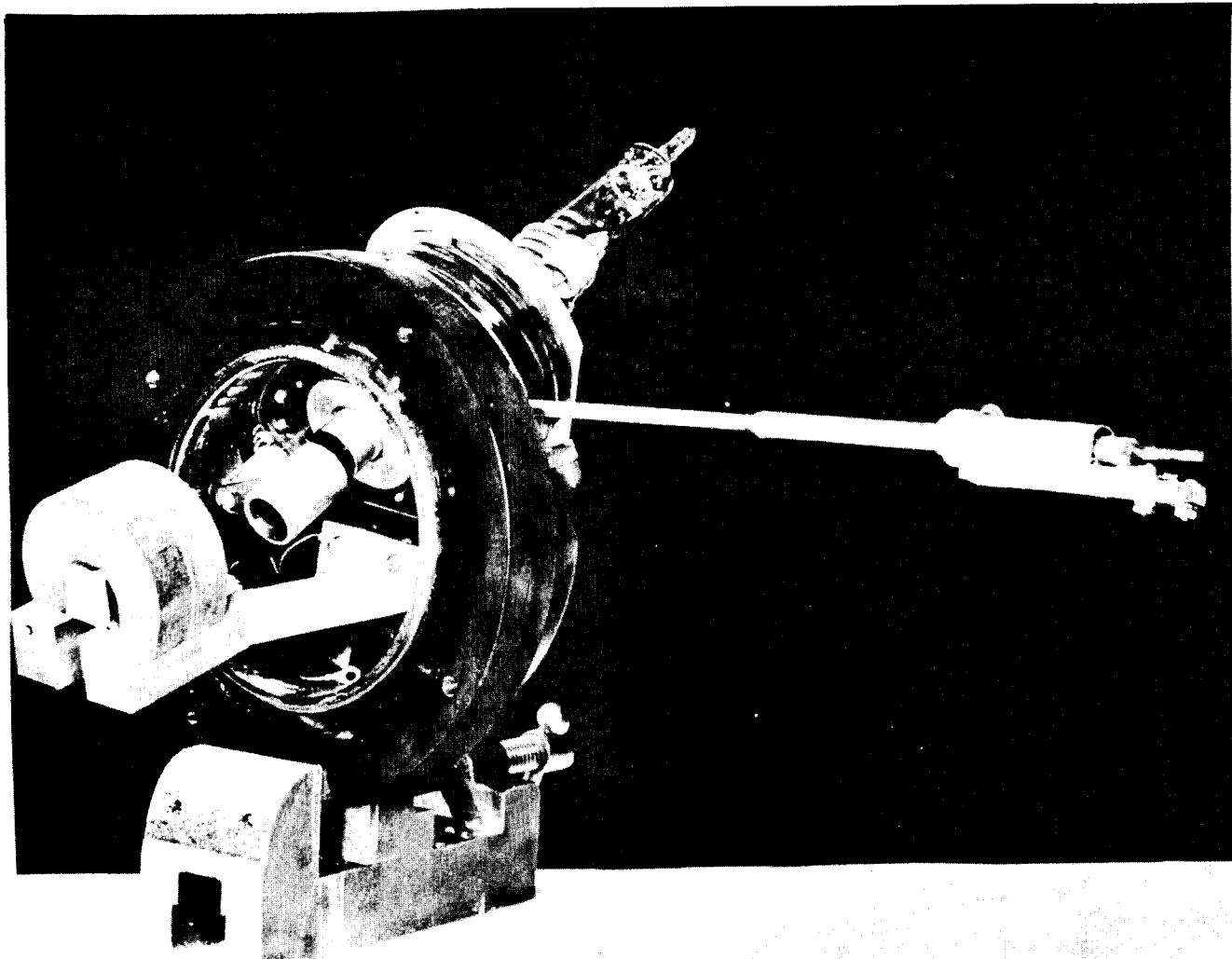


Fig. 4. Looking down the accelerator  
bore from the exit end.



ZN-692

Fig. 5. The ion source and mass separating magnet.

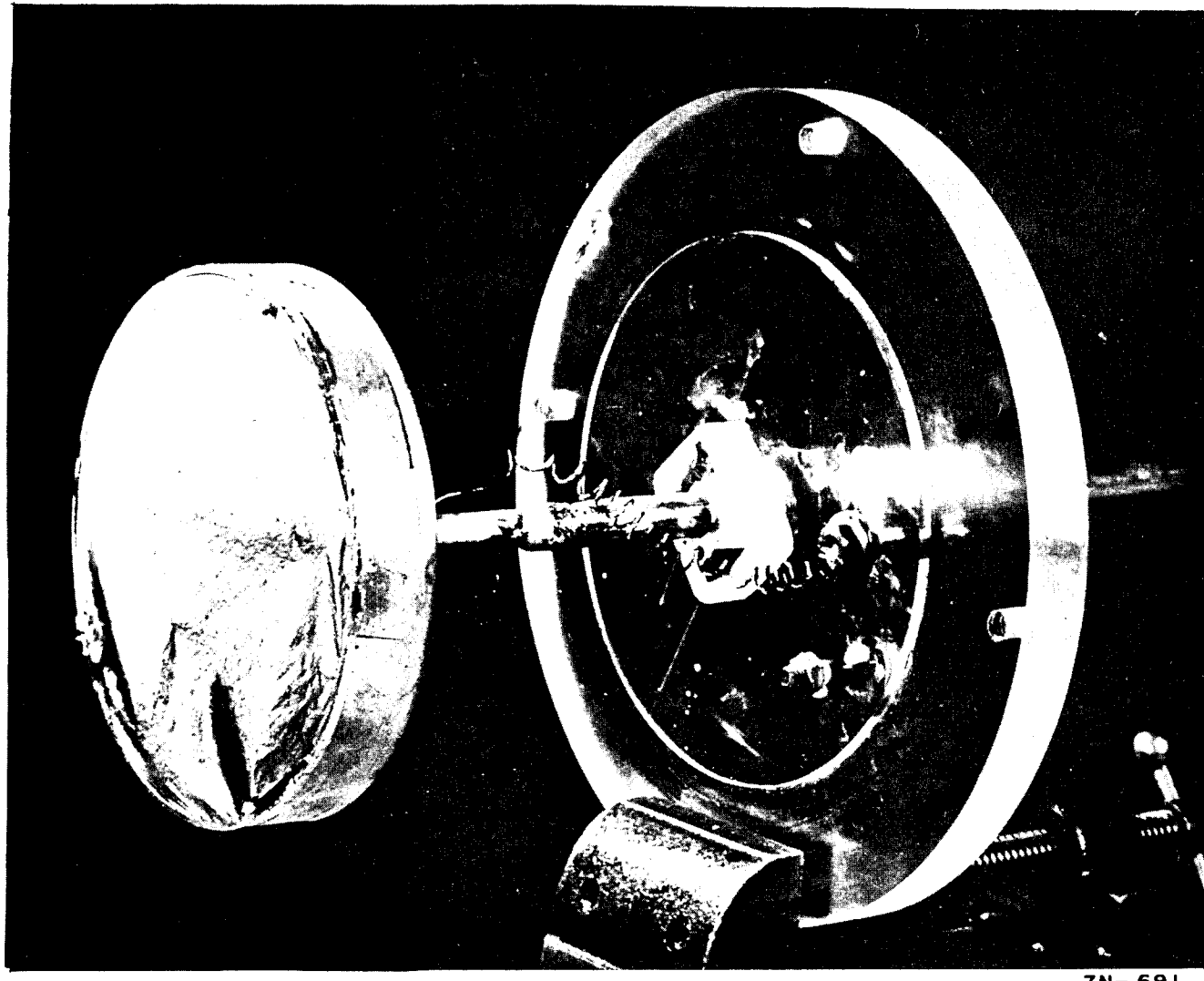


Fig. 6. Beam cup with 170 microgram/cm<sup>2</sup> Al foil.

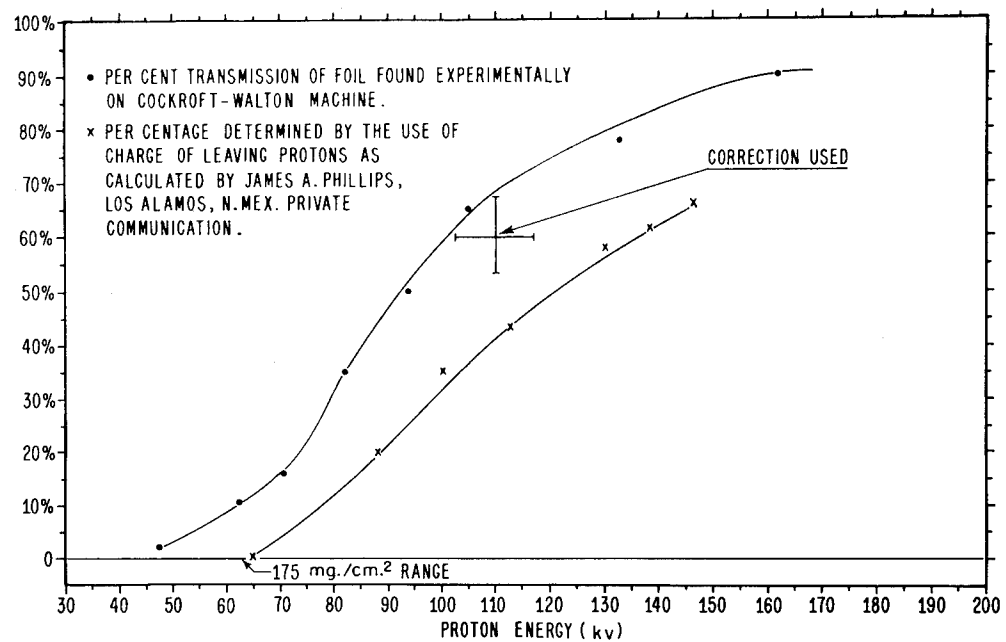


Fig. 7

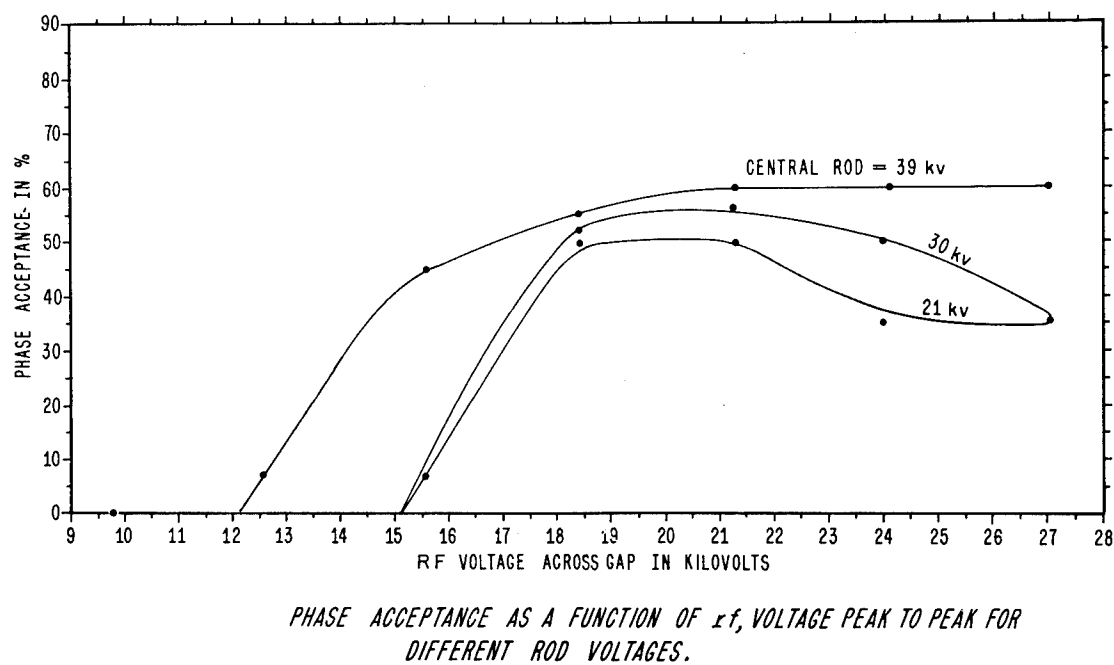
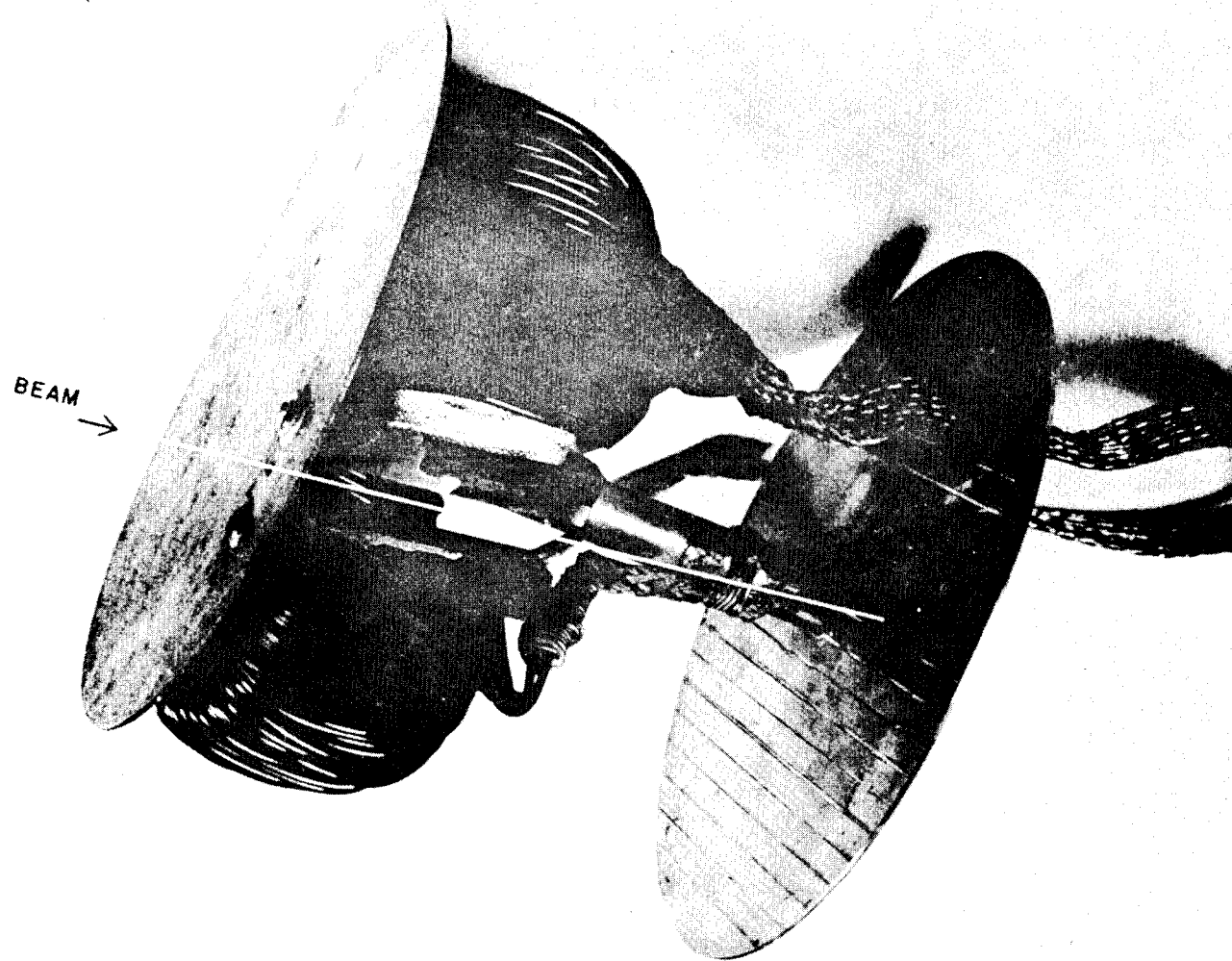
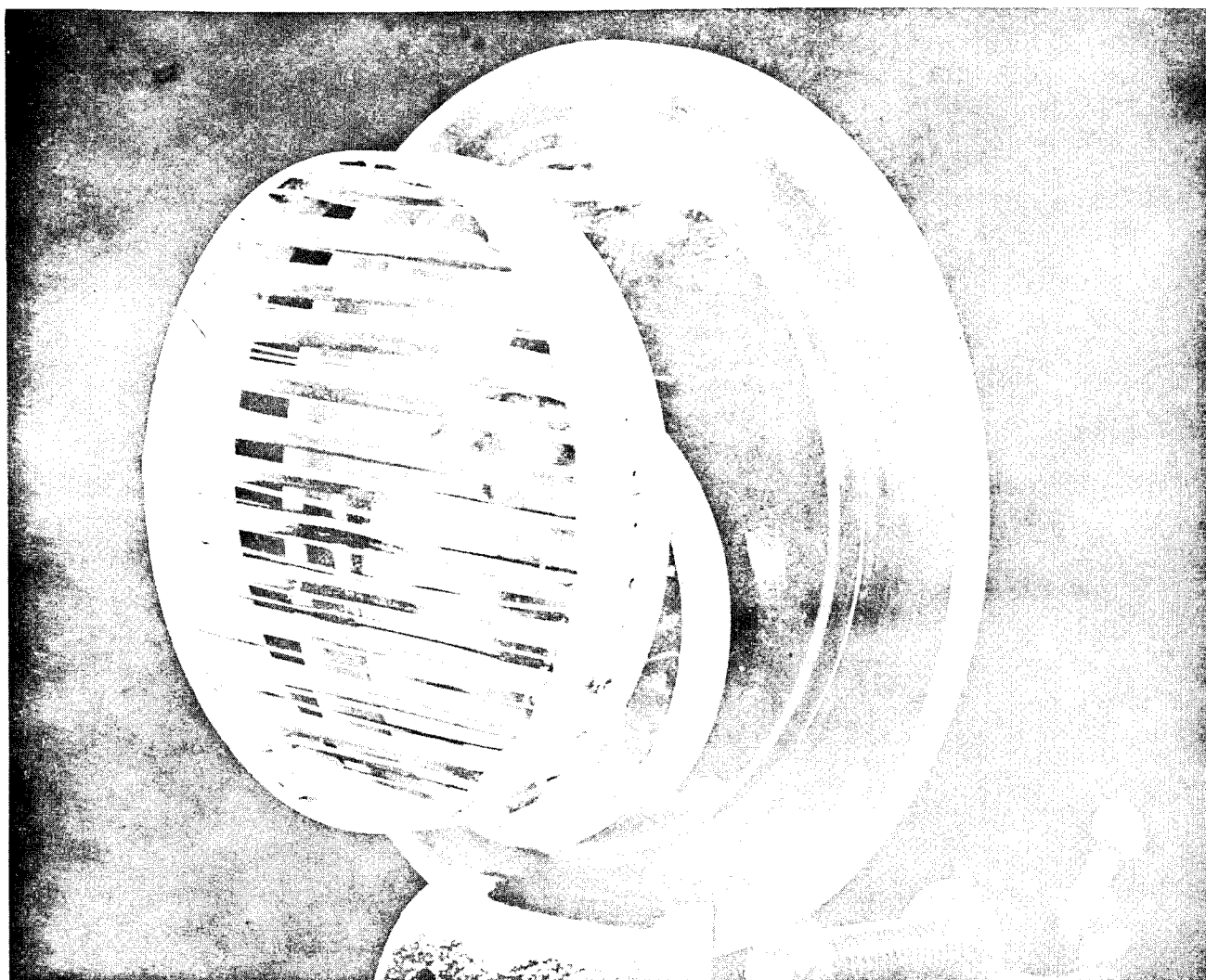


Fig. 8



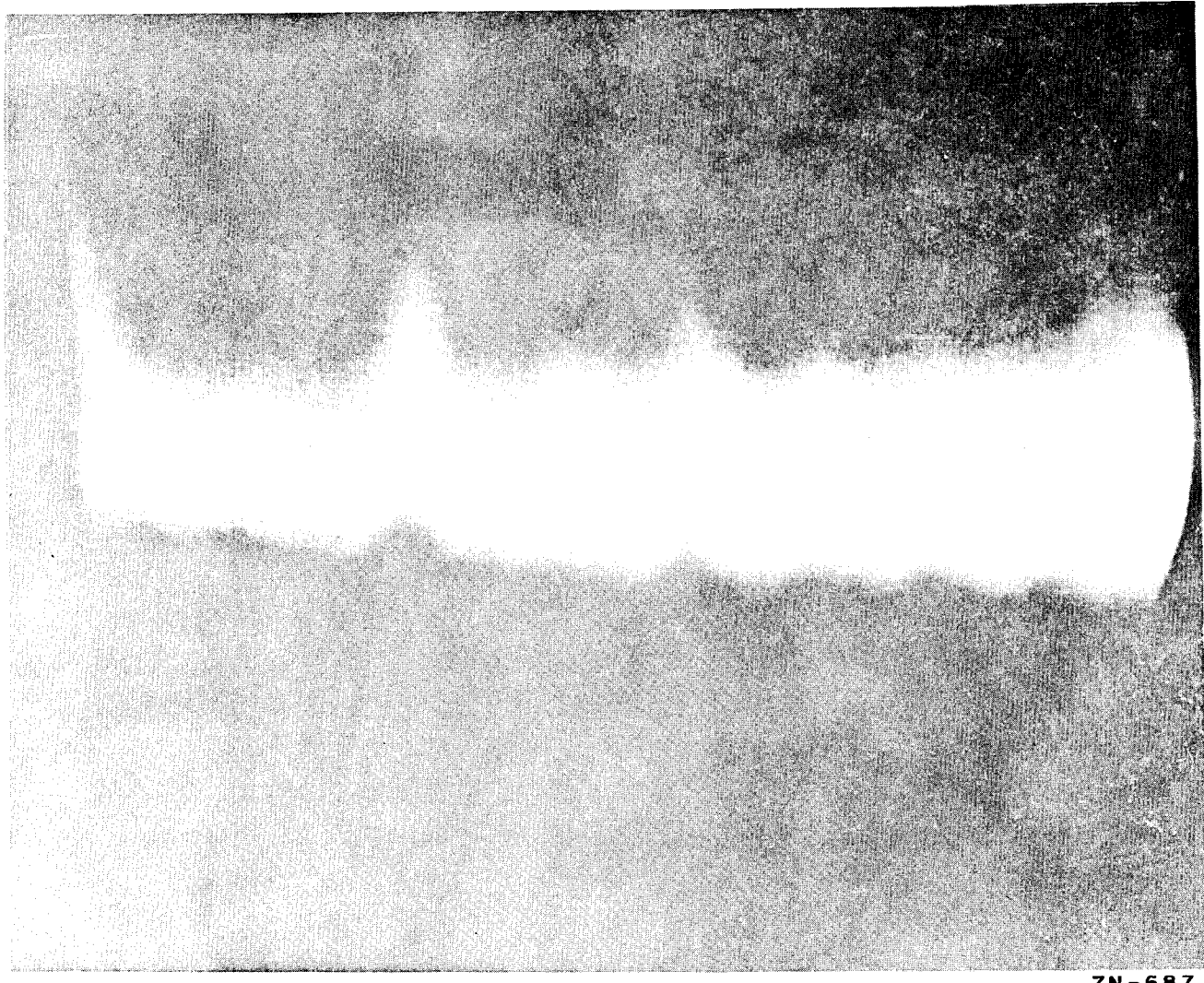
ZN - 689

Fig. 9. Beam spectrum deflecting magnet.



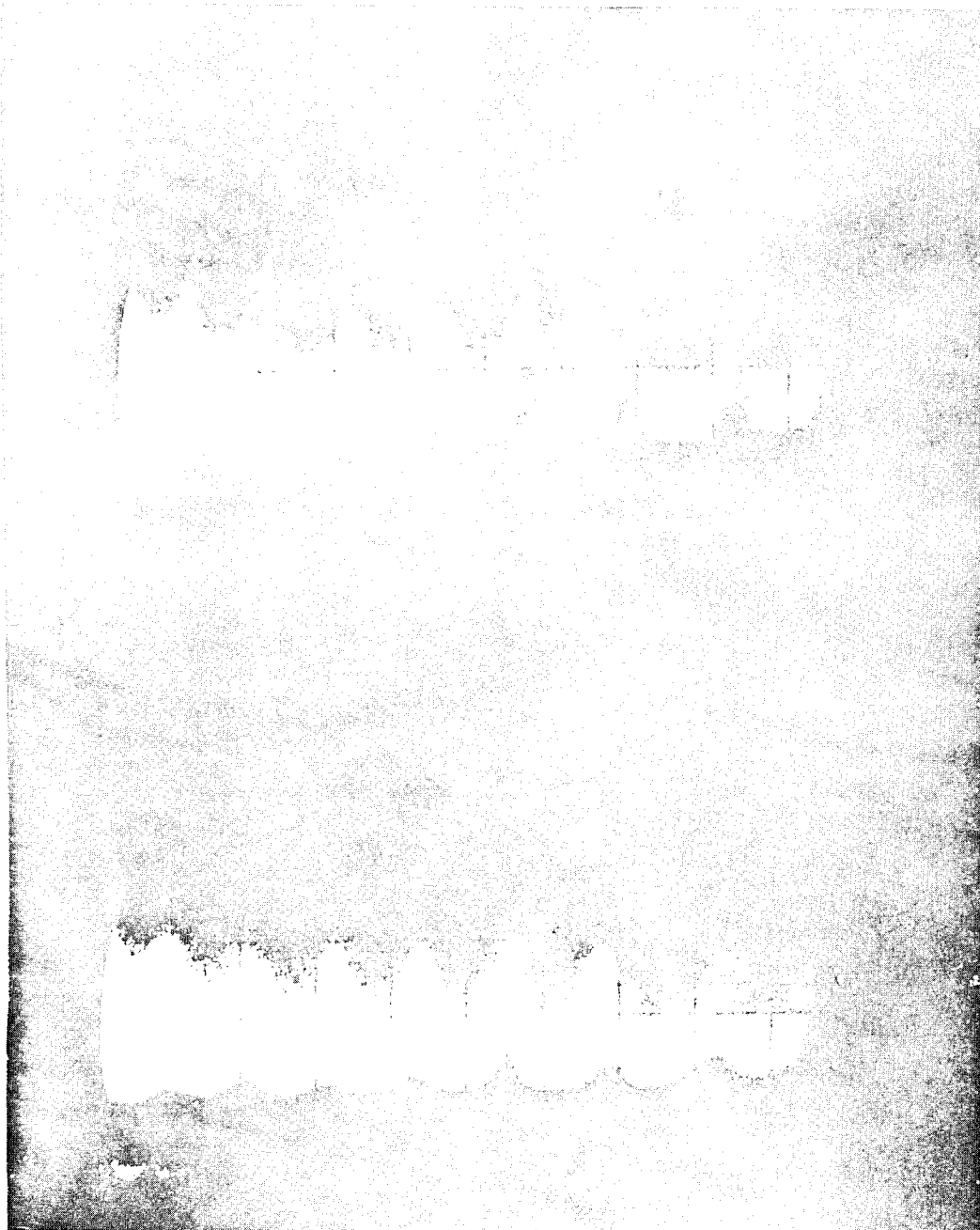
ZN - 694

Fig. 10. X-ray generating lattice.



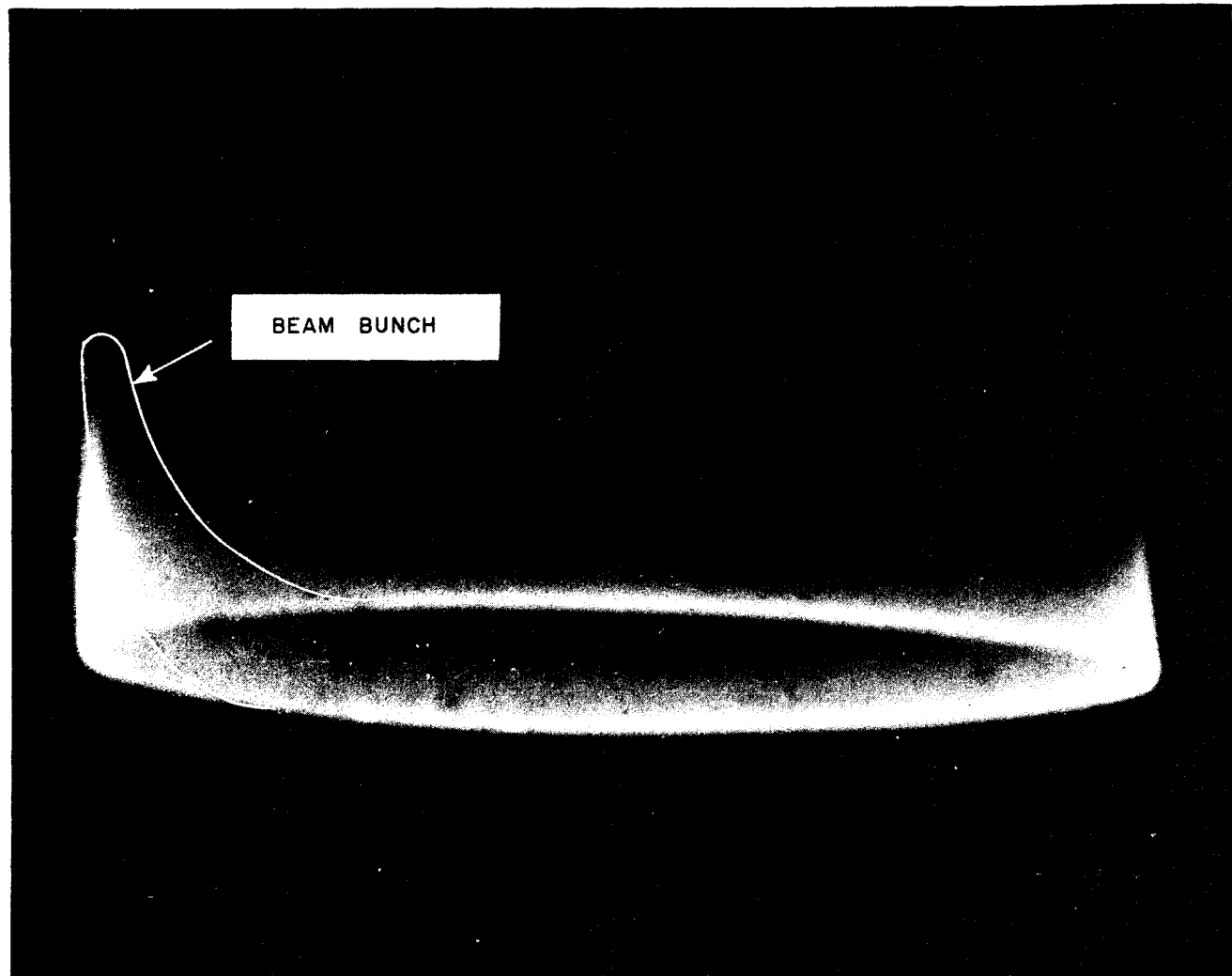
ZN-687

Fig. 11. The horizontal axis in time. The vertical axis in X-ray intensity. The Spiker arc beam pulses. Single traces showed good bunching. Trigger jitter made the composite picture broad.



ZN-686

Fig. 12. The horizontal axis is time. The vertical axis in X-ray intensity. The Spiker arc beam pulses. Single traces showed good bunching. Trigger jitter made the composite picture broad.



ZN-688

Fig. 13